Heliyon 9 (2023) e21834

Contents lists available at ScienceDirect

Heliyon

journal homepage: www.cell.com/heliyon

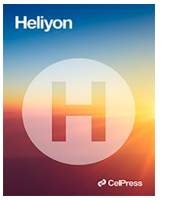

Acute and subacute hepatotoxicity of genipin in mice and its potential mechanism

Shuaikang Wang [a,1], Shuchao Ge [a,1], Yaohui Chen [c], Feng Zhou [c], Jingjing Wang [a], Liping Chen [a], Yinfang Chen [a,b], Riyue Yu [a,b], Liping Huang [a,b,*]

[a] School of Pharmacy, Jiangxi University of Chinese Medicine, Nanchang, Jiangxi, 330004, China
[b] Jiangxi Provincial Key Laboratory of Pharmacology of Traditional Chinese Medicine, Nanchang, Jiangxi, 330004, China
[c] Jiangxi Provincial People's Hospital, Nanchang, Jiangxi, 30012, China

ARTICLE INFO

Keywords:
Genipin
LD50
ANIT
Liver injury
Acute toxicity
Subacute toxicity

ABSTRACT

Gardenia, as a medicinal and edible herb, has the pharmacological activity of protecting the liver and cholagogue, but the hepatotoxicity induced by the chemical component genipin (GP) limits its application. The aim of this study was to evaluate the acute and subacute hepatotoxicity of genipin in normal mice and mice with α-naphthalene isothiocyanate (ANIT)-induced liver injury. The results of the acute study showed that the LD50 of genipin was 510 mg/kg. Genipin exhibited hepatotoxicity in normal and jaundiced mice at doses of 125 mg/kg, 250 mg/kg, and 500 mg/kg, which increased with dose. In a 28-day subacute study, the 50 mg/kg and 100 mg/kg dose groups showed some pharmacodynamic effects at 7 days but exhibited hepatotoxicity that increased with time and improved after drug withdrawal. In addition, based on proteomics, the mechanism of liver injury induced by genipin may be related to the disruption of the UDP-glucuronosyltransferase system and cytochrome P450 enzyme activity. In conclusion, this study showed that genipin hepatotoxicity was time- and dose dependent, but it is worth mentioning that hepatotoxicity was reversible. It is hoped that this study will provide a scientific basis for circumventing the adverse effects of genipin.

1. Introduction

Gardenia, as a common traditional Chinese medicine and food, is used clinically to treat various diseases, including jaundice, diarrhea and liver disease [1], and is a common traditional Chinese medicine administered for liver protection and cholagogue [2,3]. Gardenia's main active component of hepatoprotective and choleretic effects is geniposide, which has a wide range of pharmacological effects and has great development and utilization value [4–7]. Geniposide, as the main active ingredient of Gardenia with hepatoprotective and choleretic effects, is only effective by oral or duodenal administration. At the same time, geniposide is hydrolyzed as genipin under the action of intestinal flora in vivo, which is an iridoid compound and is the main form of efficacy in vivo [8–11]. Studies have shown that genipin could play a hepatoprotective role by inhibiting Fas-mediated apoptosis of rat hepatocytes and had a significant dose–response relationship [12]. In addition, genipin enhances the bile acid-independent secretory capacity of hepatocytes, mainly by stimulating exocytosis from bile canaliculi and the intercalation of multidrug resistance-associated protein 2 (Mrp2)

* Corresponding authorSchool of Pharmacy, Jiangxi University of Chinese Medicine, Nanchang, Jiangxi, 330004, China.
E-mail address: jxnchlp@163.com (L. Huang).
[1] Shuaikang Wang and Shuchao Ge have contributed equally to this work.

https://doi.org/10.1016/j.heliyon.2023.e21834
Received 29 June 2023; Received in revised form 26 October 2023; Accepted 30 October 2023
Available online 4 November 2023

as well as increasing glutathione in bile, thus exerting cholestatic effects [13].

However, studies have shown that genipin is also the toxic basis of the liver injury effect of Gardenia [13–15]. The hydrolysis of geniposide into genipin by the action of intestinal flora is considered to be one of the possible important mechanisms leading to its liver injury effects [10]. At high doses, genipin binds to some nucleophilic molecules, causing hepatotoxicity. The hydrolyzed genipin can again be spontaneously converted to dialdehyde intermediates, covalently binding to the primary amine group of free lysine residues of hepatic protein, which plays a key role in geniposide hepatotoxicity, and the toxicity is correlated with the amount of genipin after binding lysine [14].

Thus, it seems that genipin, as the pharmacodynamic basis of Gardenia jasminoides, can be regarded as a double-edged sword, having a bidirectional effect on liver protection and liver injury. To clarify whether genipin has hepatotoxicity, this study included different doses of administration according to the LD50 of genipin to investigate its acute hepatotoxicity and subacute hepatotoxicity in normal animals and to evaluate the relationship between its hepatotoxicity and dose, time and its reversible recovery degree of hepatotoxicity. However, as the material basis of the hepatoprotective and choleretic effects of Gardenia jasminoides, genipin is mostly applied to diseased organisms in the clinic [16–18], so the evaluation of its hepatotoxicity in normal animals is far from sufficient. Intrahepatic cholestasis, a common clinical disease, can eventually lead to hepatobiliary injury due to the accumulation of excessive toxic bile acids in the body [19]. Clinically, the increase in biochemical parameters, including AST, ALT, ALP, TBA, DBIL and IBIL, is a significant feature. The continuous development of cholestasis can lead to the occurrence of jaundice and, in severe cases, liver fibrosis, cirrhosis and liver failure [20], while genipin has a good therapeutic effect on cholestatic diseases [4,21,22]. Therefore, we must also clarify the following questions: Is genipin hepatoprotective or hepatotoxic in animals with disease states at the same dose? Is there a dose and time difference between hepatoprotective and hepatotoxic effects? Is the liver injury caused reversible? Therefore, in this study, we observed the changes in various liver function parameters in mice with α-naphthalene isothiocyanate (ANIT)-induced liver injury by single and multiple (3 weeks) administrations of different doses of genipin. We then evaluated whether there were differences in the dose and time of hepatoprotective and hepatotoxic effects and used proteomics to investigate the toxic mechanism of genipin, to clarify the material basis of the hepatotoxicity of Gardenia and to provide a scientific basis for its safe clinical application.

2. Materials and methods

2.1. Reagents and chemicals

Genipin was purchased from Xian Green Biological Co., Ltd. (Xian, China), and methanol and acetonitrile were obtained from Merck KGaA (Hongkong, China). Sodium carboxymethyl cellulose (CMC-Na) and phenylmethylsulfonyl fluoride (PMSF) were purchased from Solarbio (Beijing, China). ANIT and trifluoroacetic acid were purchased from Macklin Maclean Biotech Co., Ltd. (Shanghai, China). Food-grade olive oil was purchased from Yihai Grain and Oil Industry Co., Ltd. (Jiangsu, China). ALT, AST, AKP, TBIL, and HE staining solution was purchased from Nanjing Jingzhu Biotechnology Co., Ltd. (Nanjing, China). Ethanol was purchased from Hengxing Chemical Reagent Co., Ltd. (Tianjin, China). Rhamsan gum and acetone were purchased from Sinopharm Chemical Reagent Co., Ltd. (Shanghai, China). RIPA High-Efficiency Lysis Solution and BCA Protein Assay kits were purchased from Kangwei Century Biotechnology Co. (Jiangsu, China). Dithiothreitol (DTT) was purchased from Thermo Fisher Scientific (Massachusetts, USA). Indole-3-acetic acid (IAA), ammonium bicarbonate, acetic acid, and formic acid were purchased from Sigma Aldrich (St. Louis, MO, USA). Pancreatic enzymes were obtained from Madison, Wisconsin, USA).

2.2. Animals

In this study, SPF healthy Kunming mice were used, with an equal ratio of males to females and weighing 20 ± 2 g. All animals were purchased from the Laboratory Animal Center of Jiangxi University of Traditional Chinese Medicine, animal production and use license number: SCXK (Jiangxi) 2018-0003; animal quality certificate number: 0002173. Bedding and feed were provided by the Laboratory Animal Center of Jiangxi University of Traditional Chinese Medicine. All animals were maintained on a 12 h light/12 h dark cycle at 25 ± 2 C and 60 ± 20 % relative humidity with unrestricted access to a standard laboratory diet and water except during fasting periods. Animals were acclimated to this environment for 1 week prior to dosing. This study was approved by the Ethics Committee of Jiangxi University of Traditional Chinese Medicine. It was implemented in strict accordance with the Regulations of the People's Republic of China on Laboratory Animals and the Guidelines for Ethical Review of Laboratory Animal Welfare.

2.3. Selection of model concentration in the jaundice model

Forty mice were randomized according to body weight, and the grouping design was as follows: control group, 60 mg/kg ANIT group, 70 mg/kg ANIT group, and 80 mg/kg ANIT group, with 10 mice in each group. To adhere to ethical principles concerning animal research, account for substantial interindividual variability in animal experiments and consider potential attrition factors such as illness or mortality during the study, we determined a sample size of 10 animals. This sample size was selected to ensure the generation of statistically robust results. Consequently, we conducted subsequent experiments based on this sample size. After the animals were fasted for 12 h, the animals in the ANIT group were intragastrically administered the corresponding concentrations of ANIT to establish an acute jaundice model. ANIT was freshly prepared in olive oil at 6 mg/mL, 7 mg/mL and 8 mg/mL in a gavage volume of 10 mL/kg (ANIT is water insoluble but readily dissolves in oily solutions. Incorporating ANIT into olive oil enhances its bioavailability, facilitating improved gastrointestinal absorption.). The blank group was intraperitoneally injected/gavaged with the

same amount of control vehicle. Following administration, animals underwent a 12 h fasting period with unrestricted access to water. Subsequently, blood collection was performed by extracting eyeball samples. Serum was taken by standing centrifugation for biochemical index detection and analysis. The liver was taken for pathological experiments to observe the degree of lesions.

2.4. Determination of the median lethal dose in normal mice

Determination of the median lethal dose (LD50) was carried out according to the Chinese national standard method of GB15193.3–2014 [23,24]. Then, 1000 mg/kg, 500 mg/kg, 200 mg/kg, and 50 mg/kg ginipin solutions were prepared and administered by gavage to mice, and the mortality rate of animals in each group was recorded. The objective was to find and determine the range of doses that caused 0 % versus 100 % animal mortality. Based on the dose range causing 0 % and 100 % animal mortality in the experiment, five different dose groups were designed in between so that the doses were decreasing according to the equivalent ratio sequence. The time and number of animal deaths were observed and recorded for 14 consecutive days after administration. The LD50 and its 95 % confidence interval were calculated according to the modified Karber method [25–27], and the calculation formula was $\log LD_{50} = X_m - \frac{1}{2}\sum_j^i (P_j + P_{j+1})$. The experimental dose was determined according to the LD50.

2.5. Acute hepatotoxicity tests

Eighty healthy Kunming mice of SPF grade were randomly divided into groups according to body weight. The administration dose was designed according to the LD50, and the grouping design was as follows: control group, 125 mg/kg GP group, 250 mg/kg GP group, 500 mg/kg GP group, ANIT group, ANIT +125 mg/kg GP group, ANIT +250 mg/kg GP group, and ANIT +500 mg/kg GP group, with 10 animals in each group, half males and half females, housed in separate cages. The experimental design is as shown in the figure (Fig. 1). GP was dissolved in 0.5 % sodium carboxymethylcellulose solution. After fasting for 12 h, the animals in the control group were intragastrically administered blank vehicle, and the normal animals were intragastrically administered the corresponding dose of the drug. The acute jaundice model was established by intragastric administration of ANIT (70 mg/kg) in the model animals. Twelve hours after model establishment, the animals in the model group were intragastrically administered blank solvent, and each animal was intragastrically administered the corresponding dose of the drug. Within 24 h after administration, the activity, coat color, diet, excretion and death of experimental animals in each group were observed and recorded. After fasting for 12 h, following anesthesia of mice with 0.5 % pentobarbital sodium salt (IP), blood samples were collected from eyeballs and centrifuged at 3500 rpm for 15 min to obtain serum for biochemical indicators. Liver organs were excised, weighed and fixed in 10 % neutral formaldehyde for histopathological diagnosis.

2.6. Subacute hepatotoxicity test

Two hundred forty SPF healthy Kunming mice were randomly divided into 4 groups according to body weight, with 60 mice in each group, half male and half female, and intragastrically administered for 7 days, 14 days, 21 days, and 28 days according to the time

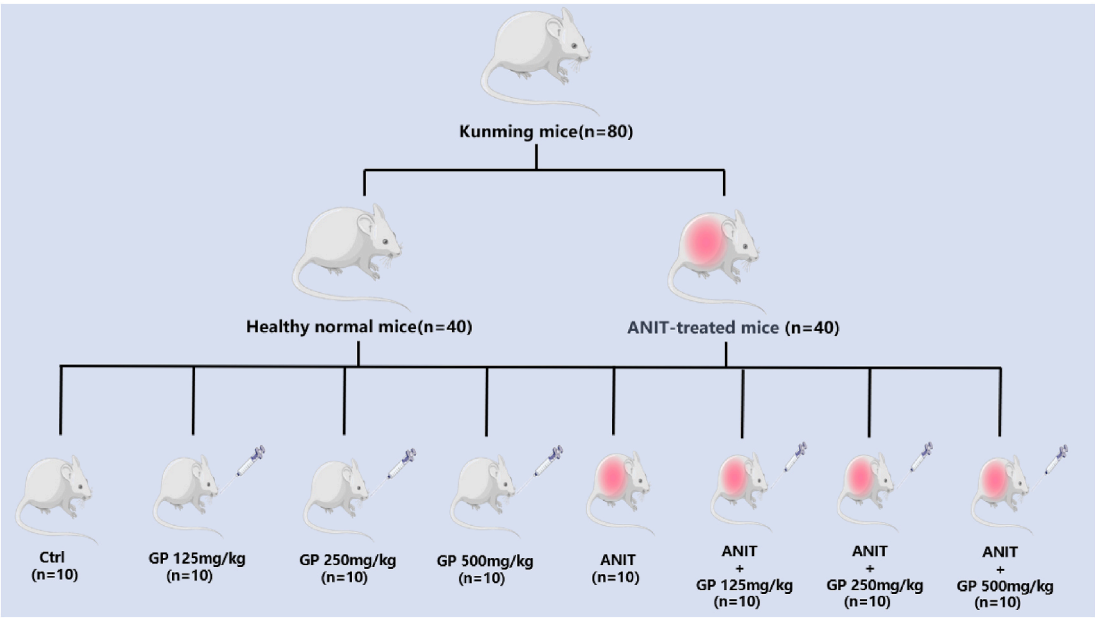

Fig. 1. Grouping of acute toxicity test animals.

points. Where Day 28 was designed as the total time to recover for 7 days following 21 days of dosing. Animals at each time point were randomly divided into 6 groups according to body weight, with 10 animals in each group, half males and half females. These groups were the control group, 50 mg/kg/d GP group, 100 mg/kg/d GP group, ANIT group, ANIT +50 mg/kg/d GP group, and ANIT +100 mg/kg/d GP group. The experimental design is as shown in the figure(Fig. 2). Animals in the control group were intragastrically administered blank vehicle, and animals in each treatment group of normal animals were intragastrically administered the corresponding dose of the drug. The acute jaundice model was established by intragastric administration of ANIT (70 mg/kg) in the model animals. Twelve hours after model establishment, the animals in the model group were intragastrically administered blank vehicle, and the animals in each treatment group were intragastrically administered the corresponding dose of the drug. Repeated ANIT interventions were required every 3 days to reinforce the model. During the administration period, the death and body weight change of animals in each group over the administration time were recorded. After the last administration, the animals were fasted for 12 h. Following anesthesia, the mice were anesthetized with 0.5 % pentobarbital sodium salt (IP). Blood samples were collected from eyeballs and centrifuged at 3500 rpm for 15 min to obtain serum for biochemical indicators. Liver organs were excised and weighed, half were fixed in 10 % neutral formaldehyde for further histopathological diagnosis, and the other half were stored in a −80 °C freezer for proteomic studies.

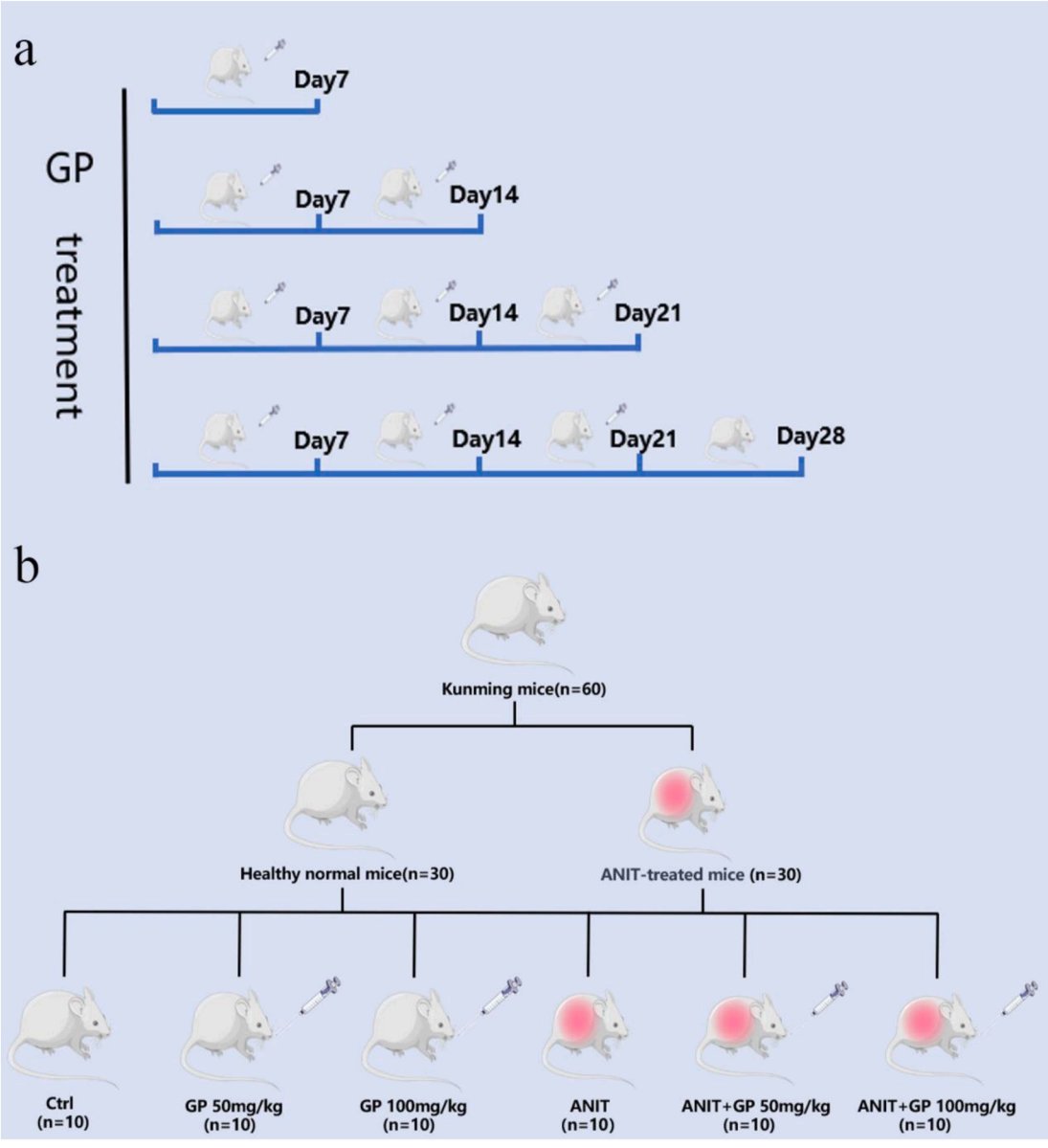

Fig. 2. (a). The administration of genipin via gastric gavage was conducted at four distinct time points: 7 days, 14 days, 21 days, and a 7-day recovery period following 21 days of dosing. (b). Grouping of animals at each time point.

2.7. Hepatic index calculation

The mouse liver index refers to the assessment of the physiological status of the mouse liver by measuring the ratio of mouse liver to body weight. Referring to the method of Yang et al. [28], after taking the liver, it was rinsed with PBS solution, the surface water was blotted with filter paper, and the liver was weighed. The calculation formula was liver index = liver weight/body weight × 100 %.

2.8. Biochemical indicators

The degree of liver injury was judged by measuring the levels of aspartate aminotransferase (AST), alanine aminotransferase (ALT), alkaline phosphatase (AKP) and total bilirubin (TBIL), which are commonly used indicators of liver injury in serum [29]. The alanine aminotransferase test kit (Cat. NO: C009-2-1), aspartate aminotransferase test kit (Cat. NO: C010-2-1), alkaline phosphatase test kit (Cat. NO: A059-2), and total bilirubin test kit (Cat. NO: C019-1-1) were purchased from Nanjing Jianjian Bioengineering Institute. The assay was performed according to the method of Duan-Yong Liu [30].

2.9. Hepatic Pathology experiments

Histopathological examination of liver tissue was performed with reference to the method of Tan et al. [31]. Tissues fixed in 10 % formalin were immersed in paraffin blocks, cut into 5-mm-thick sections, mounted on glass slides, and stained with hematoxylin and eosin (HE). Tissue sections on glass slides were observed and photographed using a light microscope (DMI3000B inverted fluorescence microscope: Leica, Germany). Changes in the histopathological features of liver tissues were classified based on the severity of four histological criteria: architecture loss, sequestration of pRBCs in microvessels, pigment deposition, and inflammation [32,33]. The histopathological scores were graded on a scale of 0–3 [nil (0), partial loss (1), moderate loss (2), and total loss (3)]. The highest possible total score was 12 (4 histological criteria × 3 as highest scale). A score of 0 means no histopathological change, and a score of 12 refers to the most severe histopathological change [33].

2.10. Liver tissue protein extraction and lysis

Liver tissue protein extraction and lysis were performed according to the method of Mullins et al. [34]. Three liver tissue samples were randomly selected from each group and quickly removed from the −80 °C freezer, and 0.1 g was weighed. We placed the tissue into the rinse solution, aspirated the water on the tissue surface, and then placed it into a 2 mL EP tube; we then placed the steel bead and added 1 mL lysis solution. All operations were performed at 4 °C. Thus, 1200×*g* was ground for 30 s and repeated twice. The EP tubes were placed in an ice box, shaken on a shaker for 40 min, placed in a high-speed centrifuge, and centrifuged at 14,000×*g* for 20 min at 4 °C, and the supernatants were taken, dispensed, and stored at −20 °C until use.

2.11. Protein quantification

Protein quantification was conducted following the methodology outlined in the study by Liao et al. [35]. The BCA protein quantitative kit's operating instructions were adhered to for the preparation of protein standards and working solutions at their designated concentrations. Subsequently, the solutions were added to a 96-well plate, and after sufficient reaction time, the absorbance was measured at a wavelength of 570 nm using a microplate reader. Subsequently, a standard curve was constructed based on the recorded absorbance values. For the protein supernatant, a 100-fold dilution was performed, followed by absorbance measurement of the diluted samples in accordance with the kit's operating instructions. Each sample was analyzed in triplicate using three wells. The resultant absorbance values were then substituted into the standard curve to ascertain the protein concentration of the sample's original solution.

2.12. Gene ontology, pathway analysis and interactions between proteins

Referring to the methodology outlined by Gato et al. [36]. Liver tissue proteins were detected using a combined Nano ESI-LC–MS system. Eggs were then subjected to identification and qualitative analysis for relative protein quantification using MaxQuant software. To further analyze the selected differential proteins, gene ontology analysis was conducted using the Metascape database (https://Metascape.org, accessed on March 3, 2023). Pathway analysis was performed utilizing the DAVID database (https://david.ncifcrf.gov/, accessed on March 3, 2023). Furthermore, network analysis was executed to assess protein–protein interactions, employing the STRING database version 11.5 (https://cn.string-db.org/, accessed on March 8, 2023).

2.13. Statistical methods

The statistical analysis was performed using the statistical package for social science (SPSS) for Windows, version 16.0 (SPSS Inc., Chicago, IL, USA). The results obtained are expressed as the mean ± SEM. One-way analysis of variance (ANOVA) and two-way ANOVA tests were used to determine significant differences between groups, and post hoc multiple comparison tests were performed using Tukey's HSD (honestly significant difference). Statistical significance was declared when the P value was less than 0.05.

3. Results

3.1. Effect of different concentrations of ANIT on liver function in mice

In comparison to the control group, significant increases in serum ALT, AST, AKP, and TBIL levels ($P < 0.01$, $P < 0.05$) were observed in animals from each dose group of ANIT (Fig. 3). Pathological liver sections revealed noteworthy liver lesions in the ANIT-exposed group compared to the control group. These lesions were characterized by localized cellular steatosis and necrosis, accompanied by inflammatory cell infiltration, cellular edema, disarrangement, and abnormal expansion of the sinusoidal space (Fig. 4a). The liver histopathology scores were analyzed as depicted in Fig. 4b. Notably, mice were intragastrically administered ANIT at a dose of 70 mg/kg, and all indicators exhibited significant differences compared to the control group ($P < 0.01$), with minimal intragroup variation. No fatalities occurred among the model animals, despite the presence of significant localized liver injury. Importantly, extensive necrosis was absent, indicating a moderate degree of modeling and a stable model condition. Therefore, the modeling concentration was selected as 70 mg/kg.

3.2. Determination of LD50 in normal mice

In the determination of the LD50, a dose range from 50 mg/kg to 1000 mg/kg was established, encompassing the entire spectrum from 0 % to 100 % mortality among animals exposed to genipin. Based on the outcomes of preliminary experiments in the genipin group, five doses were selected in equal ratio decrements within this range: 600 mg/kg, 360 mg/kg, 220 mg/kg, 130 mg/kg, and 80 mg/kg. The LD50 of genipin, along with its 95 % confidence interval, was calculated using the modified Kirschner method. The calculated LD50 for genipin was ultimately determined to be 510 mg/kg, with a 95 % confidence interval ranging from 394 to 664 mg/kg. Consequently, the doses administered in the acute toxicity test were set at 125 mg/kg, 250 mg/kg, and 500 mg/kg.

3.3. Acute hepatotoxicity of genipin in normal mice

We subsequently evaluated the hepatotoxicity of genipin in normal mice. Throughout the study period, there were no fatalities in any of the treatment groups. However, the liver index exhibited a significant increase in the groups subjected to different doses of genipin ($P < 0.01$, $P < 0.05$) (Fig. 5a), suggesting that genipin may induce hepatomegaly, hyperplasia, congestion, and edema in healthy mice. Serum biochemical parameters revealed a dose-dependent increase in ALT and AST levels in the genipin-treated group, with a notable difference observed between the 250 mg/kg and 500 mg/kg genipin groups compared to the control group ($P < 0.01$, $P < 0.05$) (Fig. 5b). In the pathological analysis, the liver tissue of the control group exhibited a normal structure. In contrast, the 125 mg/kg genipin group displayed evident inflammatory cell infiltration in the liver, accompanied by localized focal cell necrosis, extensive hepatocyte edema, and disruption of the radial arrangement of cells. Hepatocyte hydropic degeneration was notably aggravated in the 250 mg/kg genipin group, characterized by severe nucleocytoplasmic separation and an increased degeneration area. This trend persisted in the 500 mg/kg genipin group, where the degenerated nucleoplasm had essentially completely separated, and most of the cytoplasm had essentially disappeared, indicating extensive necrosis (Fig. 6a). Liver histopathology scores were analyzed, as depicted in Fig. 6b. These findings collectively suggest that genipin may induce dose-dependent hepatotoxicity in normal mice.

3.4. Subacute hepatotoxicity of genipin in normal mice

To assess the subacute hepatotoxicity of genipin in mice and evaluate the degree of reversible recovery of liver damage, we administered different doses of genipin (50 mg/kg and 100 mg/kg) to mice for durations of 7 days, 14 days, and 21 days, followed by a recovery period of 7 days.

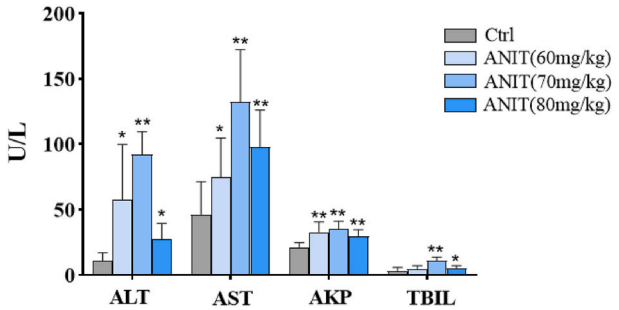

Fig. 3. Biochemical parameters in serum after single-dose oral administration of ANIT; measured markers included alanine aminotransferase (ALT), aspartate aminotransferase (AST), alkaline phosphatase (AKP) and total bilirubin (TBIL). n = 10. Data are shown as the SEM ± mean; *p < 0.05, **p < 0.01, compared with the control group.

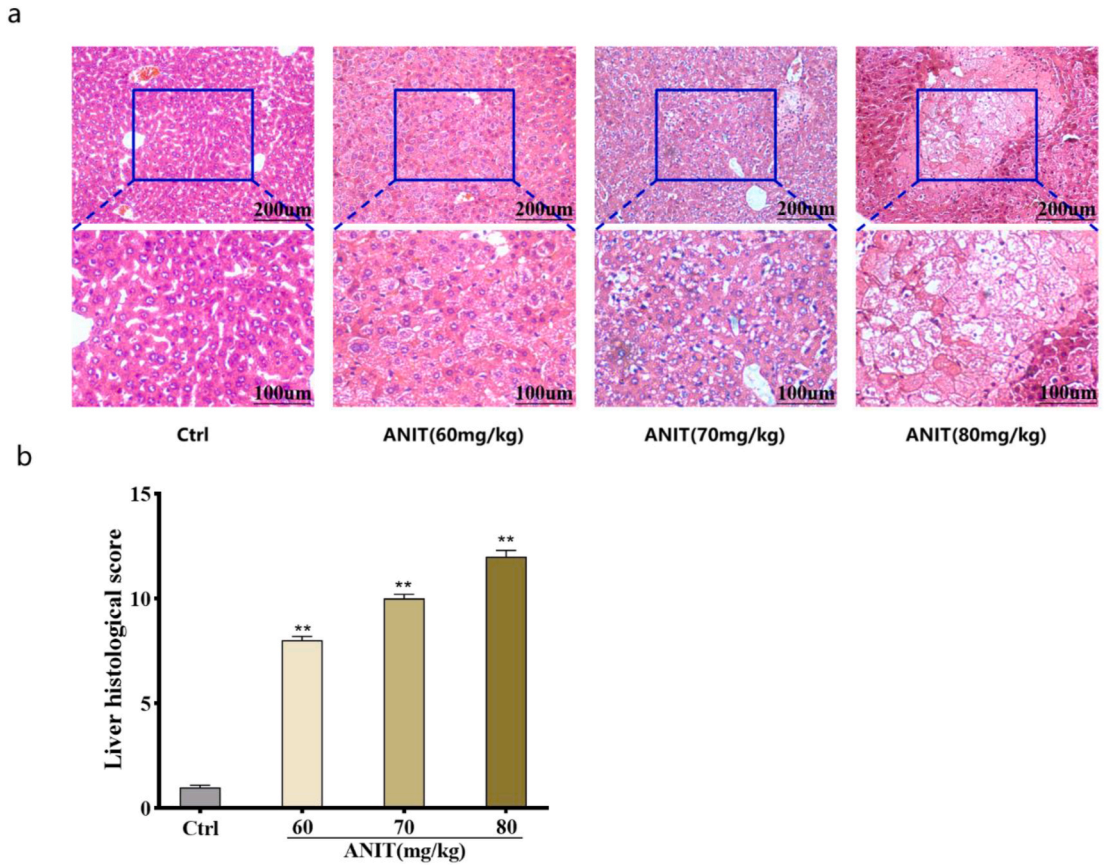

Fig. 4. (a). Representative HE images of livers of mice in different treatment groups. Animals in the ANIT group had marked liver lesions with inflammatory cell infiltration, cellular edema and abnormal dilatation of sinusoidal spaces. Arrows represent the lesion sites. Scale bar = 200 μm. (b). Histopathological score analysis of the livers. Data are shown as the SEM ± mean; **p < 0.01, compared with the control group.

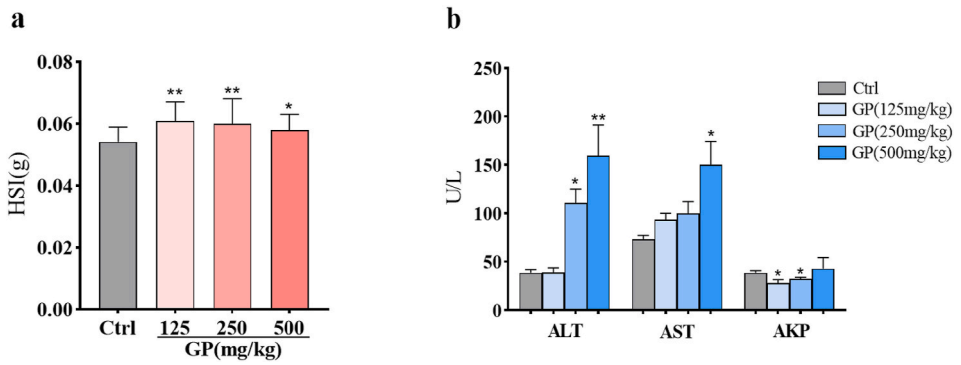

Fig. 5. (a). Effect of genipin on liver indices in normal mice. (b). Biochemical parameters in serum after single-dose oral administration of genipin. Measured markers included alanine aminotransferase (ALT), aspartate aminotransferase (AST), and alkaline phosphatase (AKP), n = 10. Data are shown as the SEM ± mean; *p < 0.05, **p < 0.01, compared with the control group.

3.4.1. Mortality and changes in body weight and liver index

Animal mortality in the low-dose genipin group primarily occurred during the initial week of treatment, whereas in the high-dose group, deaths were observed both during dosing and discontinuation, displaying no distinct pattern (Fig. 7a). The body weight of animals in the blank control group and the low-dose genipin group exhibited a continuous upward trend. In contrast, animals in the high-dose genipin group experienced a reduction in body weight over the course of administration, followed by a recovery and upward trend after the cessation of treatment (Fig. 7b). The liver index of animals in the high-dose genipin group was significantly elevated compared to that in the blank control group ($P < 0.05$), with no notable differences between the groups following the discontinuation

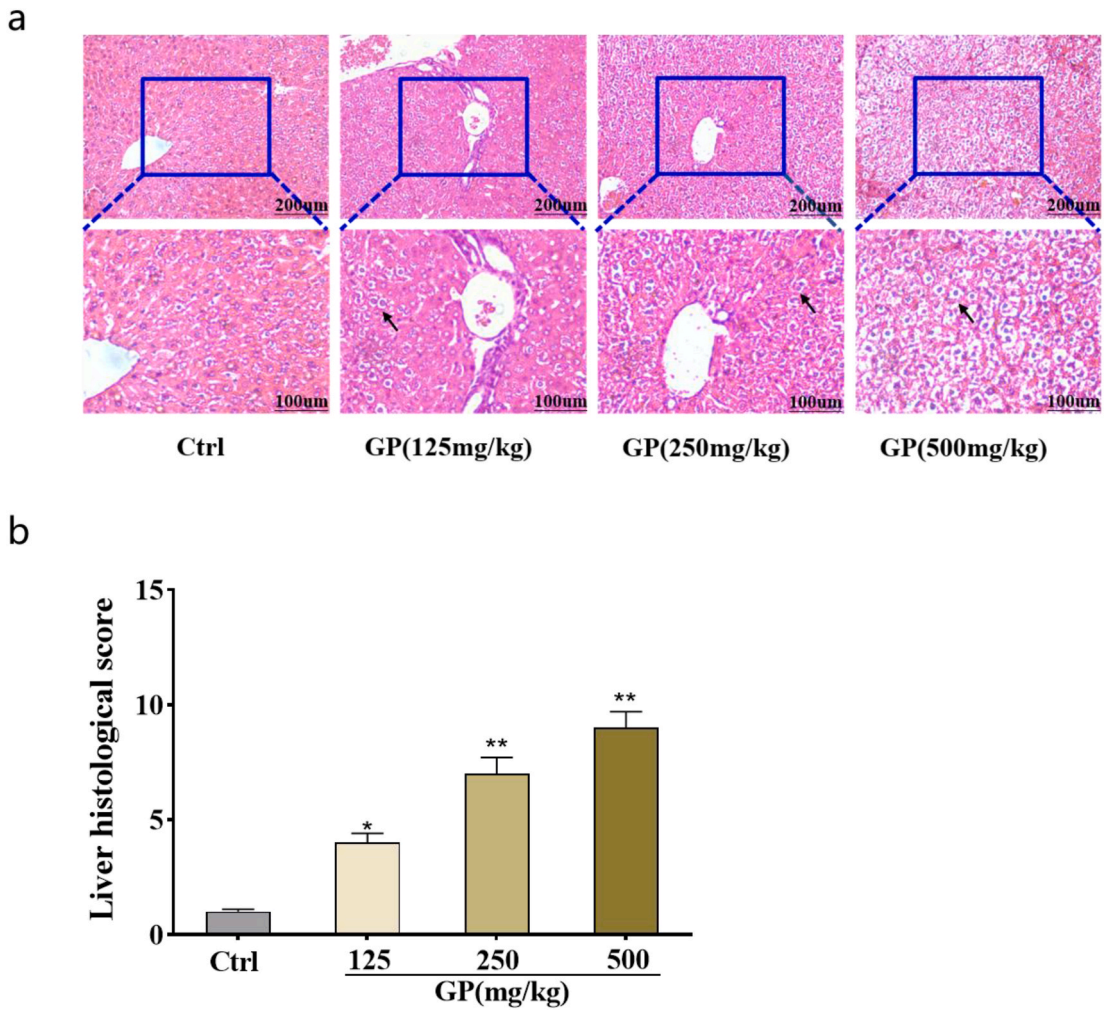

Fig. 6. (a). Representative HE images of livers of mice in different treatment groups. Liver histology was normal in the control group, hepatocytes were heavily edematous in the 125 mg/kg genipin group, and the edematous degeneration of hepatocytes increased significantly in the 250 mg/kg genipin group and continued to increase in the 500 mg/kg genipin group. Arrows indicate the site of the lesion. Scale bar = 200 μm. (b). Histopathological score analysis of the livers. Data are shown as the SEM ± mean; *p < 0.05, **p < 0.01, compared with the control group.

of treatment (Fig. 7c).

3.4.2. Effect of genipin on biochemical indices of normal mice

During the 21 days of treatment, the ALT, AST, AKP, and TBIL levels in the genipin-treated group exceeded those in the blank control group. Notably, ALT levels in the 50 mg/kg group, AST levels in the 100 mg/kg group at 14 days of dosing, and ALT levels in the 100 mg/kg group at 21 days of dosing exhibited significant increases ($P < 0.05$) (Fig. 8a). Furthermore, ALT and AST parameters displayed a time-dependent pattern, reaching their peak levels at 21 days of dosing before declining following discontinuation (Fig. 8b). These findings suggest that genipin exerts a time-dependent effect on hepatotoxicity in normal animals and that such hepatotoxicity is reversible.

3.4.3. Effect of genipin on histopathology in normal mice

In the pathological analysis, liver tissues in the control group exhibited normal structures. In the genipin-treated group, localized accumulation of inflammatory cells was observed, with a larger necrotic area and disorganized cells particularly prominent in the high-dose group. Over the course of administration, liver pathological sections from genipin-treated animals continued to display local necrosis accompanied by inflammatory cell infiltration, albeit without a significant trend of aggravation. Following a 7-day recovery period after discontinuation, the accumulation of inflammatory cells disappeared in the low-dose genipin group. However, some cells exhibited slight edema, and localized inflammatory cell infiltration persisted in the livers of animals in the high-dose genipin group, albeit with a significantly reduced necrotic area compared to that observed during administration (Fig. 9a). Liver histopathology scores are presented in Fig. 9b.

a

Group	Days(7)	Days(14)	Days(21)	Days(28)
Contrl	0	0	0	0
GP(50mg/kg)	4	0	0	0
GP(100mg/kg)	2	1	2	1

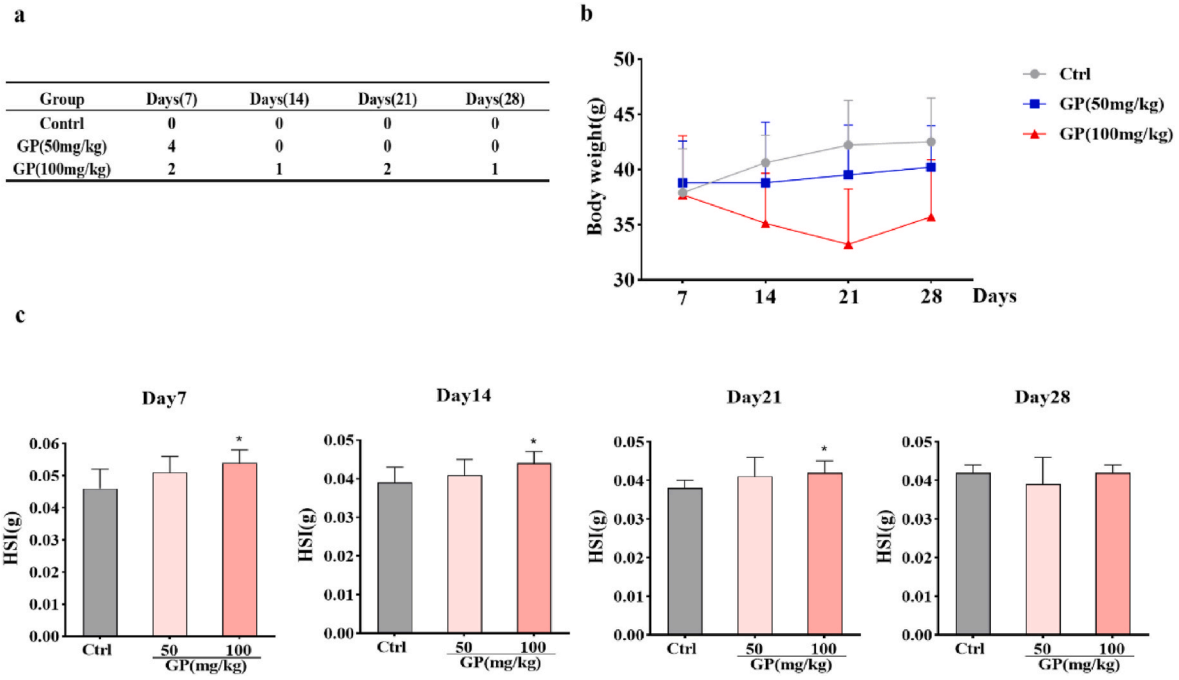

Fig. 7. Mortality and changes in body weight and liver index of normal mice during 7 days of recovery from 21 days of genipin administration. (a). Mortality in each group. (b). Trend of body weight changes in each group. (c). Effect of genipin on the liver index of normal mice. Data are shown as the SEM ± mean; *p < 0.05, compared with the control group.

3.5. Acute hepatotoxicity of genipin in mice with ANIT-induced liver injury

The aforementioned studies have demonstrated that genipin exhibits hepatotoxicity in normal mice. Consequently, our next investigation focused on whether genipin-induced hepatotoxicity at doses found effective in normal mice could impact ANIT-induced liver injury in mice. During the course of the experiment, there were instances of mortality in each group of animals (Fig. 10a). In comparison to the model group, the hepatic index significantly increased in the high-dose genipin treatment group of jaundiced animals (Fig. 10b). Serum biochemical indicators revealed that, compared to the model group, ALT and AST levels exhibited an upward trend in the genipin-treated group, but did not reach statistical significance. However, severe adverse effects were observed in animals treated with 500 mg/kg of genipin, resulting in fatalities and rendering blood sampling impractical (Fig. 10c). Histological analysis using HE staining indicated that in the model group, hepatocytes displayed disorganization, and a significant area of hepatocyte steatosis near the central vein had disappeared. The sinusoidal space appeared abnormally loose and was accompanied by inflammatory cell infiltration. In the 125 mg/kg genipin group, no extensive hepatocyte necrosis was observed, but severe cell edema was evident, and the radial arrangement of hepatocytes had disappeared, accompanied by inflammatory cell infiltration. The 250 mg/kg genipin group exhibited an increased area of steatoid necrosis of hepatocytes near the central vein, with persistent cell edema and inflammatory cell infiltration. In the 500 mg/kg genipin group, extensive inflammatory cell infiltration and obvious focal necrosis were observed. Hepatocytes in the inflammatory cell infiltration area disappeared, indicating severe liver injury (Fig. 11a). Liver histopathology scores are presented in Fig. 11b. These findings collectively suggest that genipin may exacerbate ANIT-induced liver injury.

3.6. Subacute hepatotoxicity of genipin in mice with ANIT-induced liver injury

3.6.1. Mortality and changes in body weight and liver index

Throughout the treatment period, there were fatalities among the model animals, with the majority occurring within the first week of treatment (Fig. 12a). In the initial week of treatment, all treatment groups exhibited a decline in body weight. However, both the model and low-dose genipin groups displayed a subsequent trend of weight recovery during the second week, which persisted until the conclusion of the experiment. In contrast, animals in the high-dose genipin group experienced a continual decrease in body weight until recovery following the discontinuation of treatment (Fig. 12b). The liver index results indicated that after 14 and 21 consecutive days of continuous administration, the liver index of animals in the model group significantly increased ($P < 0.05$). Conversely, the liver index of animals in the genipin treatment group exhibited a significant decrease after 7 consecutive days of continuous administration ($P < 0.05$). Animals in the high-dose genipin group showed a significant increase in the liver index after 14 and 21 consecutive days of continuous administration ($P < 0.01$, $P < 0.05$) (Fig. 12c).

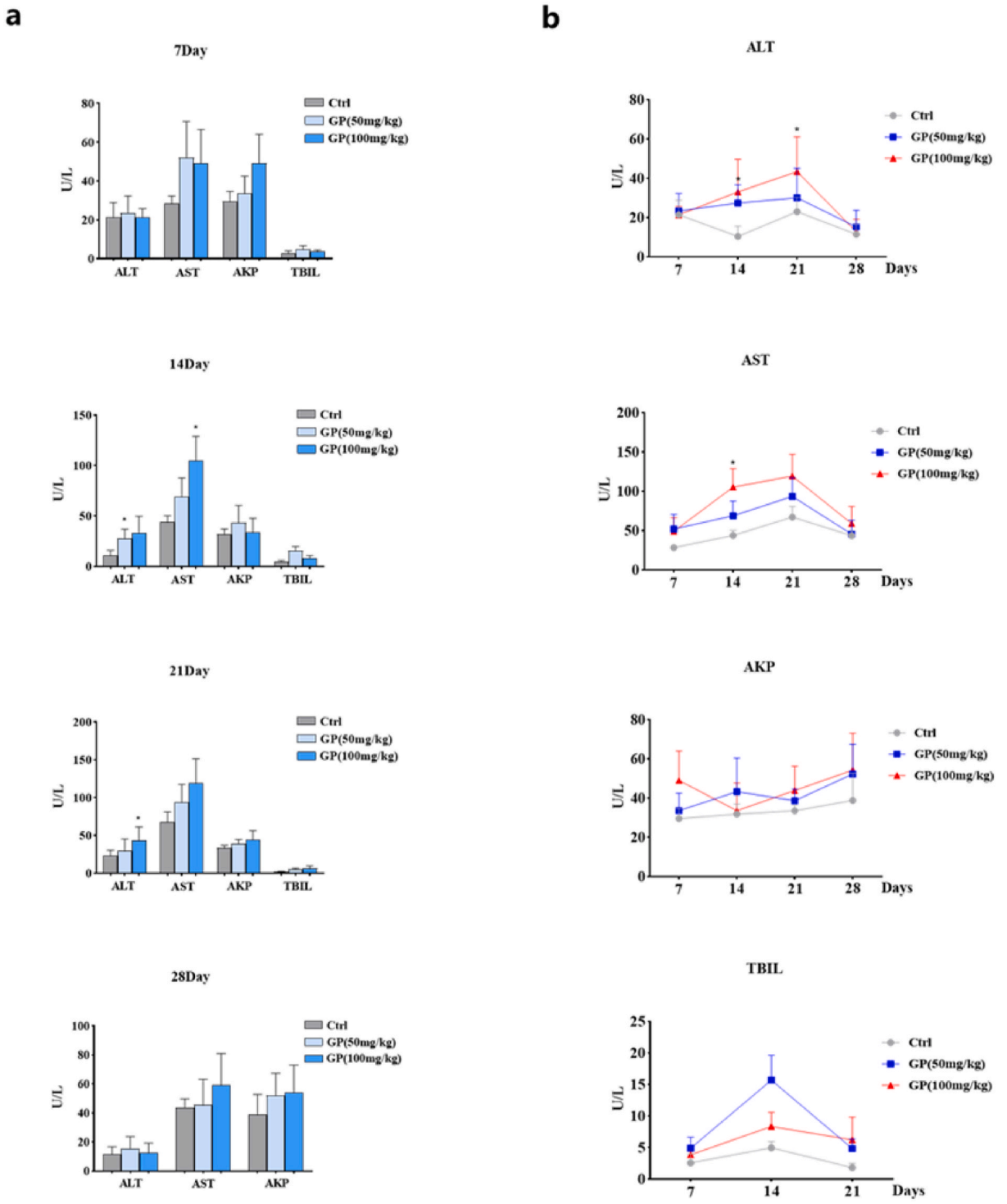

Fig. 8. (a). The levels of alanine aminotransferase (ALT), aspartate aminotransferase (AST), alkaline phosphatase (AKP), and total bilirubin (TBIL) in normal mice after taking genipin for 7 days, 14 days, 21 days, and a 7-day recovery period. (b). The changes in biochemical markers of alanine aminotransferase (ALT), aspartate aminotransferase (AST), alkaline phosphatase (AKP), and total bilirubin (TBIL) levels in normal mice after taking genipin for 21 days and during a 7-day recovery period. Data are shown as the SEM ± mean; *$p < 0.05$, compared with the control group.

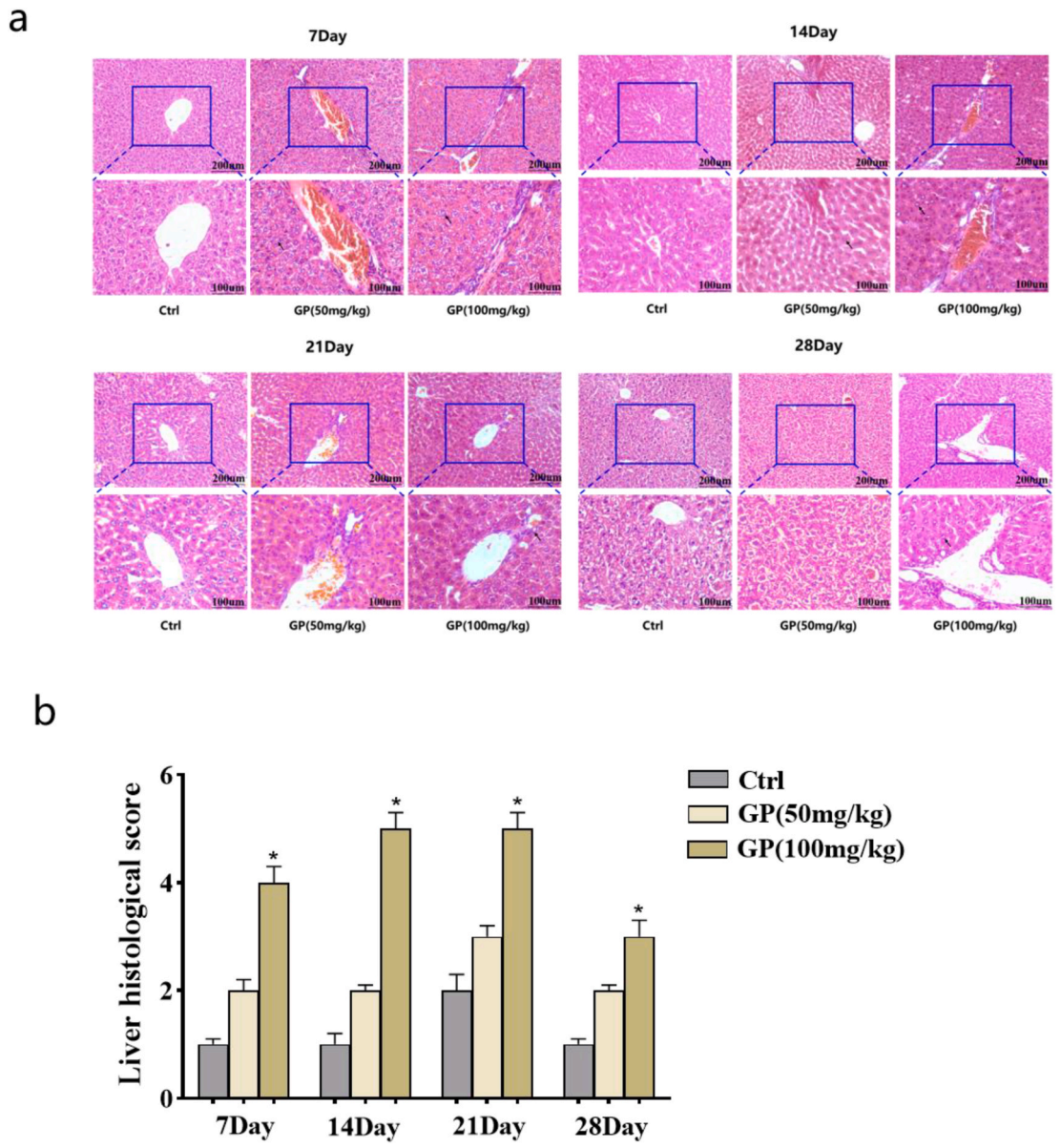

Fig. 9. (a). Representative HE images of the livers of normal mice during 7 days of recovery from 21 days of genipin administration. The control group had normal liver histology; the genipin-treated group showed localized inflammatory cell aggregation. Arrows indicate lesion sites. Scale bar = 200 μm. (b). Histopathological score analysis of the livers. Data are shown as the SEM ± mean; *p < 0.05, compared with the control group.

3.6.2. Effect of genipin on biochemical parameters in mice with ANIT-induced liver injury

The results revealed significant differences in AKP, ALT, AST, and TBIL levels between the model group and the blank control group ($P < 0.05$). After 7 days of administration, AKP, ALT, AST, and TBIL levels in genipin-treated animals fell within an intermediate range between those of the blank control group and the model group. Notably, TBIL levels were significantly different from those in the model group ($P < 0.01$, $P < 0.05$), suggesting that genipin exhibited certain pharmacodynamic effects and could alleviate liver injury symptoms in some jaundice model animals within the first 7 days of administration. In the low-dose genipin group, ALT and AST levels were higher than those in the model group at 21 days, 14 days, and 21 days, although the differences were not statistically significant. These results suggest that genipin gradually manifests its hepatotoxicity with prolonged administration, exacerbating ANIT-induced liver injury (Fig. 13a). In the genipin-treated group, ALT and AST parameters displayed a time-dependent pattern during the 21 days of dosing, reaching their peak levels at 21 days of dosing before declining following discontinuation. This indicates that genipin exhibited time-dependent hepatotoxicity in jaundiced animals, and such hepatotoxicity induced by genipin was reversible (Fig. 13b).

a

Group	Number of animals	Number of deaths	Mortality rate(%)
Model	10	2	20
GP(125mg/kg)	10	2	20
GP(250mg/kg)	10	2	20
GP(500mg/kg)	10	5	50

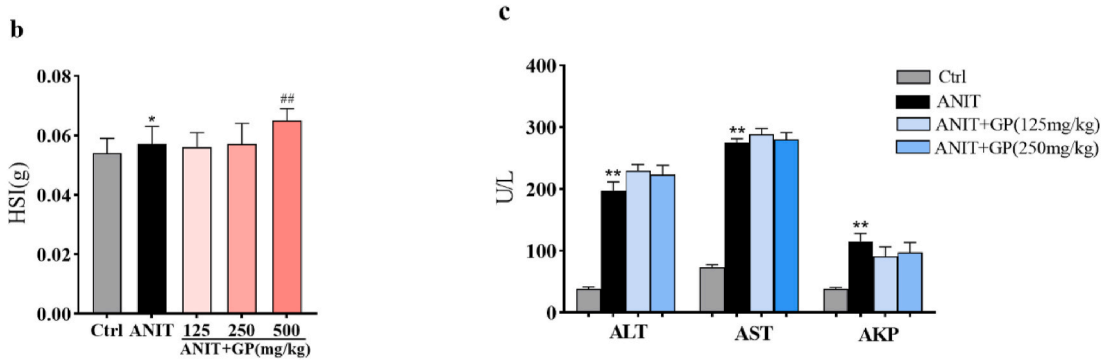

Fig. 10. Acute hepatotoxicity of genipin in mice with ANIT-induced liver injury. (a). Mortality of mice in each group. (b). Effect of genipin on the liver index in mice with ANIT-induced liver injury. (c). Biochemical parameters in serum after a single oral administration of genipin. Measured markers included alanine aminotransferase (ALT), aspartate aminotransferase (AST), and alkaline phosphatase (AKP), n = 10. Data are shown as the SEM ± mean; *p < 0.05, **p < 0.01, compared with the control group; ##p < 0.01, compared with the ANIT group.

3.6.3. Effect of genipin on histopathology of ANIT-induced liver injury in mice

In the pathological analysis, liver tissues from the blank control group exhibited a normal structure. In contrast, the livers of animals in the model group displayed extensive hepatocyte necrosis accompanied by severe inflammatory cell infiltration. The genipin-treated group demonstrated localized inflammatory cell accumulation, with a large necrotic area and disorganized cells, which were particularly pronounced in the high-dose group. Over the course of administration, liver pathological sections from genipin-treated animals continued to display local necrosis accompanied by inflammatory cell infiltration. However, this pattern did not exhibit a significant trend of aggravation. Following a 7-day recovery period after discontinuation, inflammatory cell accumulation was alleviated in the low-dose genipin group. Nonetheless, some cells exhibited slight edema, and localized inflammatory cell infiltration persisted in the livers of animals in the high-dose genipin group. Notably, the necrotic area was significantly reduced compared to that observed during the administration period (Fig. 14a). Liver histopathology scores are presented in Fig. 14b.

3.7. Proteomic studies of genipine-induced liver injury

3.7.1. Screening for differential proteins

In the subacute toxicity assessment of genipin, we observed that genipin exhibited pharmacodynamic effects at 7 days of administration, followed by toxic effects at 14 and 21 days of administration. To gain insight into the molecular mechanisms underlying GP-induced liver injury, we conducted a proteomic analysis, focusing on the 21-day administration period since the earlier subacute toxicity study did not reveal significant differences among groups after 14 days of administration.

We utilized LC–MS to collect liver tissue samples, and the resulting RAW files were subjected to proteomic identification using Protein Discovery software. From a dataset comprising 2230 screened and quantified proteins, we identified 375 dynamically changing proteins across different groups (Supplementary Fig. 1a). Subsequently, a STRING database analysis identified 51 differential proteins within the database. After excluding isolated proteins (Supplementary Fig. 1b), we identified the top ten protein interactions, including CAT, ACAA2, ADH5, CS, ACAT1, ADH1A, HADHB, ACOX1, HADHA, and ACAT2. To further characterize the expression trends of these differentially expressed proteins in mice with GP-induced liver injury, we generated a heatmap (Supplementary Fig. 1c).

3.7.2. Results of differential protein GO and KEGG analysis

Subsequent investigations aimed to assess the functions of these identified proteins. Gene Ontology (GO) analysis revealed that the molecular function and biological processes associated with the differentially expressed proteins included monocarboxylic acid metabolic processes, small molecule catabolic processes, organic hydroxy metabolic processes, oxidoreductase activities, terpenoid metabolic processes, glucuronidation, generation of cellular precursor metabolites, and energy-related processes (Supplementary Fig. 2a). Moreover, Kyoto Encyclopedia of Genes and Genomes (KEGG) pathway analysis highlighted the predominant pathways enriched among the differentially expressed proteins. These pathways included ascorbate and aldarate metabolism, synthesis and

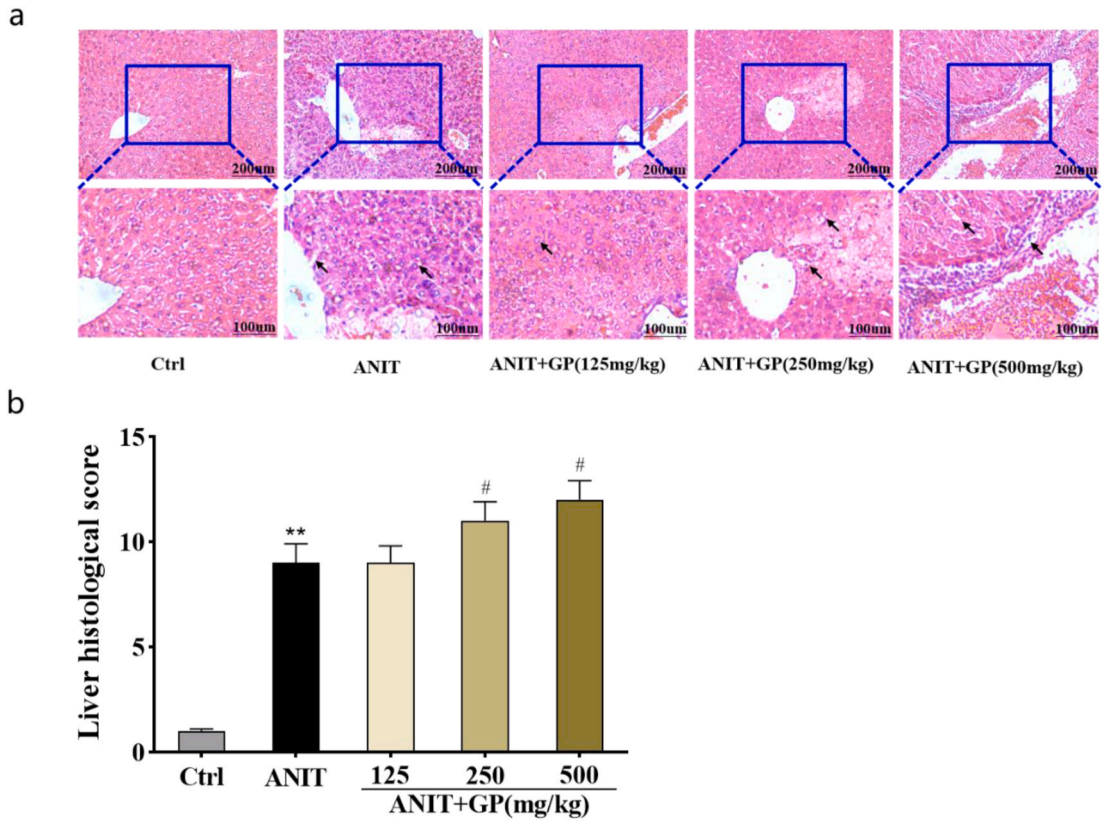

Fig. 11. (a). Representative HE images of livers of mice in different treatment groups. Animals in the model group had abnormally loose sinusoidal spaces with inflammatory cell infiltration; the 125 mg/kg genipin group had inflammatory cell infiltration; the 250 mg/kg genipin group had an increased area of steato-like necrosis of hepatocytes close to the central vein with inflammatory cell infiltration; and the 500 mg/kg genipin group had a large inflammatory cell infiltration with severe liver injury. Arrows indicate lesion sites. Scale bar = 200 μm. (b). Histopathological score analysis of the livers. Data are shown as the SEM ± mean; $^{**}p < 0.01$, compared with the control group; $\#p < 0.05$, compared with the ANIT group.

degradation of ketone metabolism, steroid hormone biosynthesis, glyoxylate and dicarboxylate metabolism, pentose and glucuronate interconversions, butanoate degradation, retinol metabolism, chemical carcinogenesis, fatty acid metabolism, and drug metabolism by cytochrome P450 (Supplementary Fig. 2b). These findings collectively suggest that GP may induce liver injury through the aforementioned signaling pathways.

4. Discussion

To comprehensively assess the hepatotoxicity of genipin, we conducted investigations into its acute and subacute hepatotoxic effects in both normal mice and jaundice model mice. The results revealed that genipin's hepatotoxicity in normal animals displayed a certain dose dependency, with higher doses exhibiting greater toxicity and, in severe cases, leading to fatalities. This outcome may be attributed to the accumulation of toxic substances from the drug in the body, which cannot be metabolized adequately. Moreover, the hepatotoxicity of genipin in normal animals exhibited a degree of time dependency. Initially, no significant differences were observed within the normal group after 7 days of administration. However, with prolonged administration, some experimental animals displayed signs of toxicity, which subsequently reverted to normal levels after discontinuation. Nevertheless, this pattern exhibited variability within the intragroup data due to substantial variations among individuals.

A subacute toxicity study conducted in jaundiced mice indicated that after 7 days of administration, genipin exhibited certain pharmacodynamic effects, mitigating liver injury symptoms in some of the jaundiced model animals. This suggests that the hepatotoxic dose of genipin in normal mice might exert a hepatoprotective effect on jaundiced mice. However, over time, genipin gradually demonstrated hepatotoxicity with a distinctive time-dependent characteristic. These findings underscore the interplay between the duration of genipin administration and its hepatoprotective and hepatotoxic effects.

The results imply that the hepatoprotective and hepatotoxic effects of genipin are intertwined with the duration of administration. It is plausible that the optimal window for the efficacy of genipin lies within the first 7 days at low doses, beyond which its toxic effects begin to manifest. Furthermore, a comparison between the results of acute and subacute toxicity in jaundiced mice indicated that genipin exhibited hepatoprotective effects at doses of 50 mg/kg and 100 mg/kg, while displaying hepatotoxicity at doses of 125 mg/kg, 250 mg/kg, and 500 mg/kg. This suggests that the hepatoprotective and hepatotoxic effects of genipin are dose dependent, and

a

Group	Days(7)	Days(14)	Days(21)	Days(28)
Contrl	0	0	0	0
ANIT	2	1	0	0
GP(50mg/kg)	6	2	3	0
GP(100mg/kg)	5	4	1	1

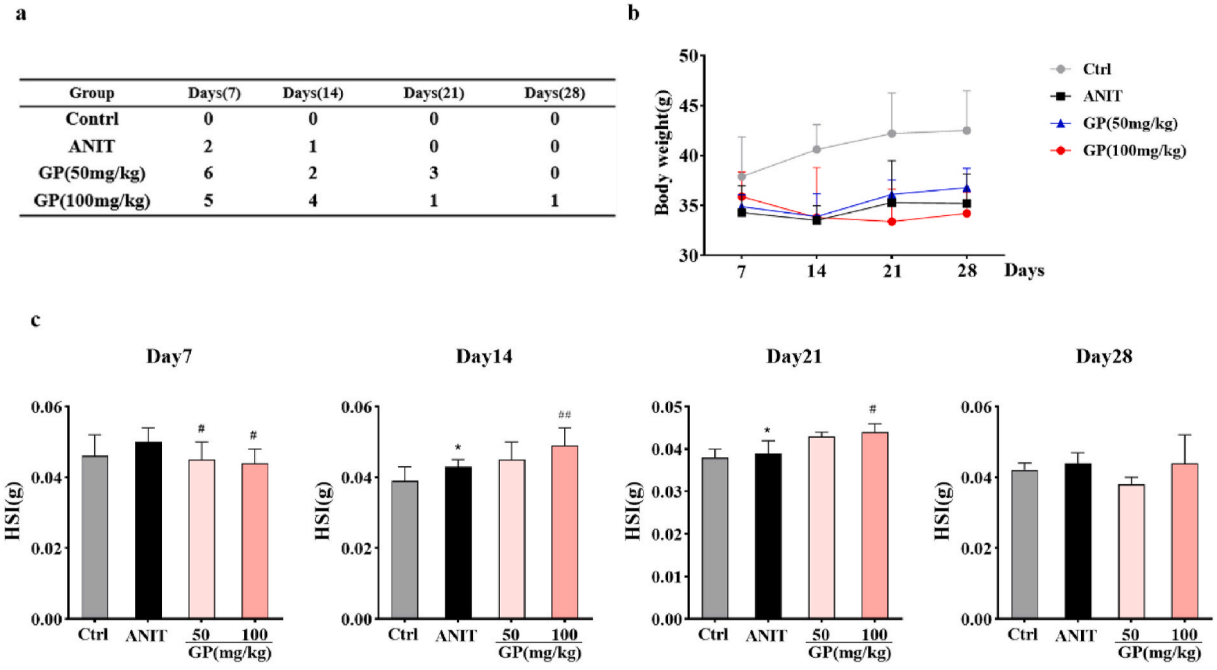

Fig. 12. Mortality and changes in body weight and liver index of ANIT-induced liver-injured mice during 7 days of recovery from 21 days of genipin administration. (a). Mortality in each group. (b). Trend of body weight changes in each group. (c). Effect of genipin on the liver index of ANIT-induced liver-injured mice. Data are shown as the SEM ± mean; *p < 0.05, compared with the control group; #p < 0.05, # #p < 0.01, compared with the ANIT group.

100 mg/kg might represent the threshold at which genipin exhibits divergent effects. Nevertheless, following the cessation of modeling and administration in all the aforementioned studies, all indicators in the experimental animals returned to normal, indicating the reversibility of genipin's hepatotoxicity in both normal animals and jaundiced model animals.

Our analysis of the relationship between differential proteins, enrichment pathways, and liver injury revealed a close connection between genipin-induced liver damage and the downregulation of key proteins in specific enrichment pathways. Here is a detailed summary of our findings. In the context of the ascorbic acid and alginate metabolic pathways, ascorbic acid primarily plays a crucial role in clearing reactive oxygen species within the body and regulating cellular functions. It also serves as a cofactor for various enzymes involved in a wide range of physiological processes, exhibiting potent antioxidant capabilities [37–40]. One of the differentially expressed proteins, Rgn, assumes a pivotal role in catalyzing the biosynthesis of ascorbic acid [41,42]. Notably, the relative expression of Rgn in the group exposed to genipin for 21 days exhibited a significant downregulation. This downregulation resulted in a reduction in ascorbic acid synthesis and, concurrently, the accumulation of hepatic neutral lipids and phospholipids [43]. Concerning UGT (uridine 5′-diphospho-glucuronosyltransferase) enzymes, Ugt1a2, Ugt1a9, and Ugt2a1 belong to the UGT class of proteases, which are involved in catalyzing phase II biotransformation reactions. These reactions entail the conjugation of lipophilic substrates with glucuronic acid, increasing the water solubility of metabolites and facilitating their excretion through urine or bile. Proper elimination and removal of drugs, endogenous compounds, and xenobiotics are intimately tied to the functionality of UGTs [44,45]. Hence, the downregulation of UGT family protein expression seems to disrupt the normal metabolism of drugs, leading to the accumulation of drug toxicity and consequent hepatotoxicity. Cyp2a12, Cyp2c39, Cyp2c68, Cyp3a41a, and Cyp4a12a are members of the cytochrome P450 enzyme family. These proteins are predominantly expressed in the liver and play a pivotal role in xenobiotic metabolism. Members of the cytochrome P450 family facilitate the conversion of xenobiotics, including drugs, into polar compounds through various reactions, such as oxidation, reduction, hydrolysis, and binding, ultimately resulting in their excretion from the body [46–48]. In the context of retinol metabolism, Cyp2a12, Cyp2c39, Cyp2c68, and Cyp3a41a primarily catalyze the conversion of retinoic acid to 4-hydroxy-retinoic acid, a critical step in the normal metabolism of retinol within the body. The downregulation of these proteins inhibits the retinol metabolism process, ultimately negatively impacting the organism. Furthermore, CYP enzymes play crucial roles in ascorbic acid metabolism, steroid biosynthesis, and fatty acid metabolism [48,49]. In summary, our findings suggest that genipin-induced liver injury is closely associated with the downregulation of key proteins in the aforementioned pathways. Typically, the toxicity of a drug decreases as it undergoes metabolism. However, the inhibition of protein activity leads to the accumulation of toxic components of the drug in the body, resulting in toxicity. Under normal circumstances, the levels of substances such as ascorbic acid, retinol, steroids, and fatty acids should remain within a relatively stable range. When proteins related to metabolism are expressed abnormally, it eventually leads to the abnormal accumulation or insufficient synthesis of these substances in the body, causing harm.

Our research has unequivocally demonstrated that the hepatotoxicity of genipin exhibits characteristics of both time and dose

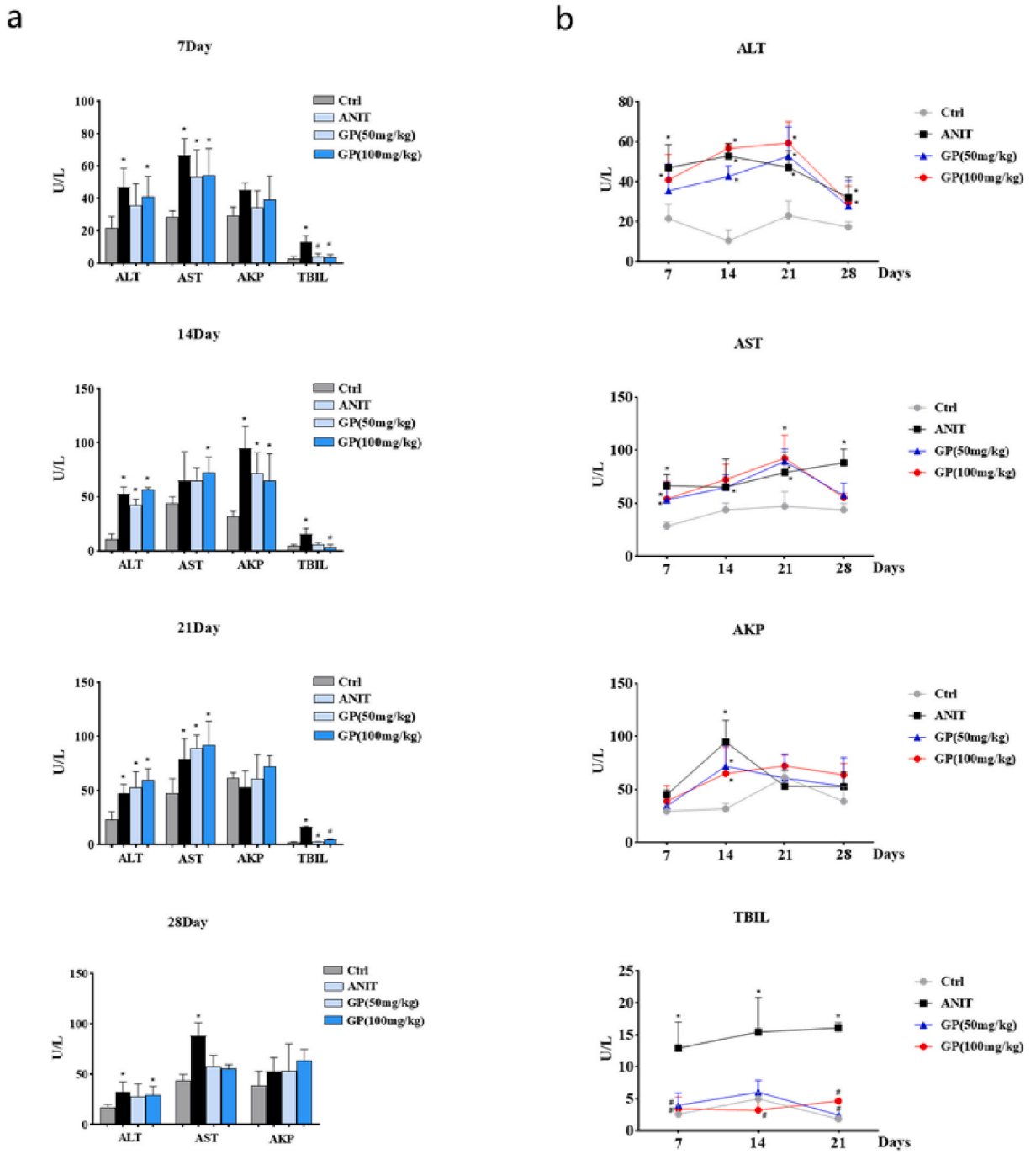

Fig. 13. (a). The levels of alanine aminotransferase (ALT), aspartate aminotransferase (AST), alkaline phosphatase (AKP), and total bilirubin (TBIL) in ANIT-induced liver injury mice after taking genipin for 7 days, 14 days, 21 days, and during a 7-day recovery period. (b). The changes in biochemical markers, including alanine aminotransferase (ALT), aspartate aminotransferase (AST), alkaline phosphatase (AKP), and total bilirubin (TBIL), in ANIT-induced liver injury mice after taking genipin for 21 days and during a 7-day recovery period. Data shown are SEM ± mean; *p < 0.05, compared with the Control group; #p < 0.05, compared with the ANIT group.

dependency, a finding of significant importance. Nevertheless, we acknowledge certain limitations within our study. Notably, we have yet to determine the precise dosage and time standards governing genipin-induced liver injury, necessitating further in-depth research and validation. In summary, we aspire for our research outcomes to serve as a scientific foundation for the effective prevention and management of adverse liver reactions caused by genipin. Furthermore, we hope to stimulate future investigations delving deeper into this issue; this, in turn, will aid in the establishment of more explicit drug guidance principles, ensuring the safe and effective use of

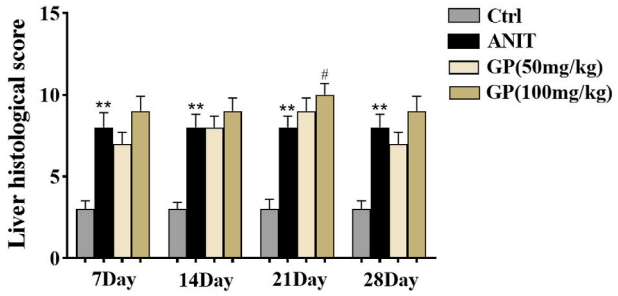

Fig. 14. (a). Representative HE images of livers of ANIT-induced mice during 7 days of recovery from 21 days of genipin administration. The control group had normal liver histology; the model group had severe inflammatory cell infiltration; the genipin-treated group showed localized inflammatory cell aggregation, and the high-dose group had a large necrotic area with disorganized cells. Arrows indicate lesion sites. Scale bar = 200 μm. (b). Histopathological score analysis of the livers. Data are shown as the SEM ± mean; $^{**}p < 0.01$, compared with the control group; $\#p < 0.05$, compared with the ANIT group.

genipin.

5. Conclusion

The results obtained in our study reveal that the hepatotoxicity of genipin exhibits both dose dependency and time dependency. The underlying mechanism of this hepatotoxicity may be associated with disruptions in the activity of UDP-glucuronosyltransferases and cytochrome P450 enzymes. Importantly, the liver toxicity induced by genipin is reversible. These findings hold promise in effectively preventing adverse liver reactions caused by genipin and provide a scientific foundation for addressing related issues.

Funding statement

This work was supported by Jiangxi University of Chinese Medicine Science and Technology In-novation Team Development Program (CXTD22007), National Key Research and Development Program Project (2019YFC1604905) and Special Scientific Research Fund Project for First-class Disci-pline of Traditional Chinese Medicine in Jiangxi Province (JXSYLXK-ZHYAO137). This project is also funded by the State Administration of Traditional Chinese Medicine of Jiangxi University of Chinese Medicine Key Discipline Cultivation Discipline of Traditional Chinese Medicine Pharmacology of Traditional Chinese Medicine.

Data availability statement

The data that support the findings of this study are available upon request. Please feel free to reach out for access to the data.

Ethics approval

This study was reviewed and approved by Jiangxi University of Chinese Medicine's ethics committee, with the approval number: [JZLLSC 2019-391].

CRediT authorship contribution statement

Shuaikang Wang: Conceptualization, Data curation, Formal analysis, Methodology, Project administration, Writing – original draft, Writing – review & editing. **Shuchao Ge:** Data curation. **Yaohui Chen:** Data curation. **Feng Zhou:** Project administration. **Jingjing Wang:** Investigation. **Liping Chen:** Software. **Yinfang Chen:** Investigation. **Riyue Yu:** Data curation. **Liping Huang:** Data curation, Methodology, Project administration, Writing – review & editing.

Declaration of competing interest

The authors declare that they have no known competing financial interests or personal relationships that could have appeared to influence the work reported in this paper.

Appendix A. Supplementary data

Supplementary data to this article can be found online at https://doi.org/10.1016/j.heliyon.2023.e21834.

References

[1] P. Chen, Y. Chen, Y. Wang, S. Cai, L. Deng, J. Liu, H. Zhang, Comparative evaluation of hepatoprotective activities of geniposide, crocins and crocetin by CCl4-induced liver injury in mice, Biomolecules & therapeutics 24 (2) (2016) 156–162, https://doi.org/10.4062/biomolther.2015.094.

[2] J. Tian, S. Qin, J. Han, J. Meng, A. Liang, A review of the ethnopharmacology, phytochemistry, pharmacology and toxicology of Fructus Gardeniae (Zhi-zi), J. Ethnopharmacol. 289 (2022), 114984, https://doi.org/10.1016/j.jep.2022.114984.

[3] L. Chen, M. Li, Z. Yang, W. Tao, P. Wang, X. Tian, X. Li, W. Wang, Gardenia jasminoides Ellis: ethnopharmacology, phytochemistry, and pharmacological and industrial applications of an important traditional Chinese medicine, J. Ethnopharmacol. 257 (2020), 112829, https://doi.org/10.1016/j.jep.2020.112829.

[4] L. Wang, G. Wu, F. Wu, N. Jiang, Y. Lin, Geniposide attenuates ANIT-induced cholestasis through regulation of transporters and enzymes involved in bile acids homeostasis in rats, J. Ethnopharmacol. 196 (2017) 178–185, https://doi.org/10.1016/j.jep.2016.12.022.

[5] Y. Zhou, R. Zhang, K. Rahman, Z. Cao, H. Zhang, C. Peng, Diverse Pharmacological Activities and Potential Medicinal Benefits of Geniposide. *Evidence-Based Complementary and Alternative Medicine : eCAM*, 2019, https://doi.org/10.1155/2019/4925682, 2019:4925682.

[6] S. Gao, Q. Feng, The beneficial effects of geniposide on glucose and lipid metabolism: a review, Drug Des. Dev. Ther. 16 (2022) 3365–3383, https://doi.org/10.2147/dddt.S378976.

[7] L. Liu, Q. Wu, Y. Chen, G. Gu, R. Gao, B. Peng, Y. Wang, A. Li, J. Guo, X. Xu, X. Shao, L. Li, Y. Shen, J. Sun, Updated pharmacological effects, molecular mechanisms, and therapeutic potential of natural product geniposide, Molecules 27 (10) (2022), https://doi.org/10.3390/molecules27103319.

[8] J. Kim, H. Kim, S. Lee, Protective effects of geniposide and genipin against hepatic ischemia/reperfusion injury in mice, Biomolecules & therapeutics 21 (2) (2013) 132–137, https://doi.org/10.4062/biomolther.2013.005.

[9] K. Ueno, Y. Takeda, Y. Iwasaki, F. Yoshizaki, Simultaneous estimation of geniposide and genipin in mouse plasma using high-performance liquid chromatography, Anal. Sci. : the international journal of the Japan Society for Analytical Chemistry 17 (10) (2001) 1237–1239, https://doi.org/10.2116/analsci.17.1237.

[10] Kobashi Akao, Aburada, Enzymic studies on the animal and intestinal bacterial metabolism of geniposide, Biol. Pharm. Bull. (1994), https://doi.org/10.1248/bpb.17.1573.

[11] S. Habtemariam, G. Lentini, Plant-Derived anticancer agents: lessons from the pharmacology of geniposide and its aglycone, genipin, Biomedicines 6 (2) (2018), https://doi.org/10.3390/biomedicines6020039.

[12] M. Yamamoto, N. Miura, N. Ohtake, S. Amagaya, A. Ishige, H. Sasaki, Y. Komatsu, K. Fukuda, T. Ito, K. Terasawa, Genipin, a metabolite derived from the herbal medicine Inchin-ko-to, and suppression of Fas-induced lethal liver apoptosis in mice, Gastroenterology 118 (2) (2000) 380–389, https://doi.org/10.1016/s0016-5085(00)70220-4.

[13] J. Shoda, T. Miura, H. Utsunomiya, K. Oda, M. Yamamoto, M. Kano, T. Ikegami, N. Tanaka, H. Akita, K. Ito, H. Suzuki, Y. Sugiyama, Genipin enhances Mrp2 (Abcc2)-mediated bile formation and organic anion transport in rat liver, Hepatology 39 (1) (2004) 167–178, https://doi.org/10.1002/hep.20003.

[14] Y. Li, H. Pan, X. Li, N. Jiang, L. Huang, Y. Lu, F. Shi, Role of intestinal microbiota-mediated genipin dialdehyde intermediate formation in geniposide-induced hepatotoxicity in rats, Toxicol. Appl. Pharmacol. 377 (2019), 114624, https://doi.org/10.3390/molecules24213920.

[15] Y. Hou, S. Tsai, P. Lai, Y. Chen, P. Chao, Metabolism and pharmacokinetics of genipin and geniposide in rats, Food Chem. Toxicol. : an international journal published for the British Industrial Biological Research Association 46 (8) (2008) 2764–2769, https://doi.org/10.1016/j.fct.2008.04.033.

[16] M. Mikami, H. Takikawa, Effect of genipin on the biliary excretion of cholephilic compounds in rats, Hepatol. Res. : the official journal of the Japan Society of Hepatology 38 (6) (2008) 614–621, https://doi.org/10.1111/j.1872-034X.2007.00309.x.

[17] Y. Yen, W. Chen, S. Hayakawa, C. Chien, In-chern-hau-tang and genipin reduces acute urinary bladder distension evoked sympathetic activation-induced hepatic dysfunction in rats, Am. J. Chin. Med. 37 (2) (2009) 339–349, https://doi.org/10.1142/s0192415x09006886.

[18] S. Takeuchi, T. Goto, K. Mikami, K. Miura, S. Ohshima, K. Yoneyama, M. Sato, T. Shibuya, D. Watanabe, E. Kataoka, D. Segawa, A. Endo, W. Sato, R. Yoshino, S. Watanabe, Genipin prevents fulminant hepatic failure resulting in reduction of lethality through the suppression of TNF-alpha production, Hepatol. Res.: the official journal of the Japan Society of Hepatology 33 (4) (2005) 298–305, https://doi.org/10.1016/j.hepres.2005.08.009.

[19] Q. Meng, X.L. Chen, C.Y. Wang, Q. Liu, H.J. Sun, P.Y. Sun, X.K. Huo, Z.H. Liu, J.H. Yao, K.X. Liu, Alisol B 23-acetate protects against ANIT-induced hepatotoxity and cholestasis, due to FXR-mediated regulation of transporters and enzymes involved in bile acid homeostasis, Toxicol. Appl. Pharmacol. 283 (3) (2015) 178–186, https://doi.org/10.1016/j.taap.2015.01.020.

[20] J. Boyer, New perspectives for the treatment of cholestasis: lessons from basic science applied clinically, J. Hepatol. 46 (3) (2007) 365–371, https://doi.org/10.1016/j.jhep.2006.12.001.

[21] J. Shoda, T.M. H. Utsunomiya, et al., Genipin enhances Mrp2 (Abcc2)-mediated bile formation and organic anion transport in rat liver, Hepatology (2004), https://doi.org/10.1002/hep.20003.

[22] K. Okada, J. Shoda, M. Kano, S. Suzuki, N. Ohtake, M. Yamamoto, H. Takahashi, H. Utsunomiya, K. Oda, K. Inchinkoto Sato, A herbal medicine and its ingredients dually exert Mrp2/MRP2-mediated choleresis and Nrf2-mediated antioxidative action in rat liver, Am. J. Physiol. Gastrointest. Liver Physiol. 292 (5) (2007) 1450–1463, https://doi.org/10.1152/ajpgi.00302.2006.

[23] Y. Zhang, R. Tian, H. Wu, X. Li, L. Bian, Evaluation of acute and sub-chronic toxicity of Lithothamnion sp. in mice and rats, Toxicol Rep 7 (2020), https://doi.org/10.1016/j.toxrep.2020.07.005.

[24] X. Xu, J. Wang, D. Zhang, W. Feng, W. Song, [Safety toxicological evaluation of wen radix codonopsis], Wei sheng yan jiu = Journal of hygiene research 50 (6) (2021) 1012–1018, https://doi.org/10.19813/j.cnki.weishengyanjiu.2021.06.023.

[25] H. Jung, S. Choi, Sequential method of estimating the LD50 using a modified up-and-down rule, J. Biopharm. Stat. 4 (1) (1994) 19–30, https://doi.org/10.1080/10543409408835069.

[26] Q. Zhao, Z. Yang, S. Cao, Y. Chang, Y. Cao, J. Li, Z. Yao, Y. Wen, X. Huang, R. Wu, Q. Yan, Y. Huang, X. Ma, X. Han, Y. Wu, Acute oral toxicity test and assessment of combined toxicity of cadmium and aflatoxin B in kunming mice, Food Chem. Toxicol. : an international journal published for the British Industrial Biological Research Association 131 (2019), 110577, https://doi.org/10.1016/j.fct.2019.110577.

[27] X. Zhang, F. Liu, B. Chen, Y. Li, Z. Wang, Acute and subacute oral toxicity of polychlorinated diphenyl sulfides in mice: determining LD50 and assessing the status of hepatic oxidative stress, Environ. Toxicol. Chem. 31 (7) (2012) 1485–1493, https://doi.org/10.1002/etc.1861.

[28] Q. Yang, R. Xie, X. Geng, X. Luo, B. Han, M. Cheng, Effect of Danshao Huaxian capsule on expression of matrix metalloproteinase-1 and tissue inhibitor of metalloproteinase-1 in fibrotic liver of rats, World J. Gastroenterol. 11 (32) (2005) 4953–4956, https://doi.org/10.3748/wjg.v11.i32.4953.

[29] M. McGill, The past and present of serum aminotransferases and the future of liver injury biomarkers, EXCLI journal 15 (2016) 817–828, https://doi.org/10.17179/excli2016-800.

[30] B. Zhou, H. Zhao, X. Lu, W. Zhou, F. Liu, X. Liu, D. Liu, Effect of puerarin regulated mTOR signaling pathway in experimental liver injury, Front. Pharmacol. 9 (2018) 1165, https://doi.org/10.3389/fphar.2018.01165.

[31] Z. Tan, A. Liu, M. Luo, X. Yin, D. Song, M. Dai, P. Li, Z. Chu, Z. Zou, M. Ma, B. Guo, B. Chen, Geniposide inhibits alpha-naphthylisothiocyanate-induced intrahepatic cholestasis: the downregulation of STAT3 and NF[formula: see text]B signaling plays an important role, Am. J. Chin. Med. 44 (4) (2016) 721–736, https://doi.org/10.1142/s0192415x16500397.

[32] P. Viriyavejakul, V. Khachonsaksumet, C. Punsawad, Liver changes in severe Plasmodium falciparum malaria: histopathology, apoptosis and nuclear factor kappa B expression, Malar. J. 13 (2014) 106, https://doi.org/10.1186/1475-2875-13-106.

[33] S. Fazalul Rahiman, R. Basir, H. Talib, T. Tie, Y. Chuah, M. Jabbarzare, W. Chong, M. Mohd Yusoff, N. Nordin, M. Yam, W. Abdullah, R. Abdul Majid, Interleukin-27 exhibited anti-inflammatory activity during Plasmodium berghei infection in mice, Trop. Biomed. 30 (4) (2013) 663–680, 10.1179/2047772413Z.000000000180.

[34] Y. Mullins, K. Keogh, G. Blackshields, D. Kenny, A. Kelly, S. Waters, Transcriptome assisted label free proteomics of hepatic tissue in response to both dietary restriction and compensatory growth in cattle, J. Proteonomics 232 (2021), 104048, https://doi.org/10.1016/j.jprot.2020.104048.

[35] L. Chen-Chung, C. Yen-Shuo, C. Wan-Chun, T. Yu-Tang, C. Hsiao-Li, W. Jyh-Horng, H. Chi-Chang, Proteomics analysis to identify and characterize the molecular signatures of hepatic steatosis in ovariectomized rats as a model of postmenopausal status, Nutrients 7 (10) (2015) 8752–8766.
[36] W. Gato, J. Wu, I. Appiah, O. Smith, H. Rochani, Hepatic proteomic assessment of oral ingestion of titanium dioxide nano fiber (TDNF) in Sprague Dawley rats, J. Environ. Sci. Health - Part A Toxic/Hazard. Subst. Environ. Eng. 57 (2022) 1116–1123, https://doi.org/10.1080/10934529.2022.2159733.
[37] A. Carr, S. Maggini, Vitamin C and immune function, Nutrients 9 (11) (2017), https://doi.org/10.3390/nu9111211.
[38] L. Fransson, K. Mani, Novel aspects of vitamin C: how important is glypican-1 recycling? Trends Mol. Med. 13 (4) (2007) 143–149, https://doi.org/10.1016/j.molmed.2007.02.005.
[39] T. Ishikawa, S. Shigeoka, Recent advances in ascorbate biosynthesis and the physiological significance of ascorbate peroxidase in photosynthesizing organisms, Biosci. Biotechnol. Biochem. 72 (5) (2008) 1143–1154, https://doi.org/10.1271/bbb.80062.
[40] V. Kumar, A. Rani, A.K. Dixit, D. Pratap, D. Bhatnagar, A comparative assessment of total phenolic content, ferric reducing-anti-oxidative power, free radical-scavenging activity, vitamin C and isoflavones content in soybean with varying seed coat colour, Food Res. Int. 43 (1) (2010) 323–328, https://doi.org/10.1016/j.foodres.2009.10.019.
[41] Y. Kondo, Y. Inai, Y. Sato, S. Handa, S. Kubo, K. Shimokado, S. Goto, M. Nishikimi, N. Maruyama, A. Ishigami, Senescence marker protein 30 functions as gluconolactonase in L-ascorbic acid biosynthesis, and its knockout mice are prone to scurvy, Proc. Natl. Acad. Sci. U. S. A. 103 (15) (2006) 5723–5728, https://doi.org/10.1073/pnas.0511225103.
[42] N. Aranibar, V. Bhaskaran, K. Ott, J. Vassallo, D. Nelson, L. Lecureux, L. Gong, S. Stryker, L. Lehman-McKeeman, Modulation of Ascorbic Acid Metabolism by Cytochrome P450 Induction Revealed by Metabonomics and Transcriptional Profiling. Magnetic Resonance in Chemistry, MRC, 2009, pp. S12–S19, https://doi.org/10.1002/mrc.2503.
[43] A. Ishigami, Y. Kondo, R. Nanba, T. Ohsawa, S. Handa, S. Kubo, M. Akita, N. Maruyama, SMP30 deficiency in mice causes an accumulation of neutral lipids and phospholipids in the liver and shortens the life span, Biochem. Biophys. Res. Commun. 315 (3) (2004) 575–580, https://doi.org/10.1016/j.bbrc.2004.01.091.
[44] M. Perreault, L. Gauthier-Landry, J. Trottier, M. Verreault, P. Caron, M. Finel, O. Barbier, The Human UDP-glucuronosyltransferase UGT2A1 and UGT2A2 enzymes are highly active in bile acid glucuronidation, Drug Metabol. Dispos.: the biological fate of chemicals 41 (9) (2013) 1616–1620, https://doi.org/10.1124/dmd.113.052613.
[45] N. Sneitz, M. Vahermo, J. Mosorin, L. Laakkonen, D. Poirier, M. Finel, Regiospecificity and stereospecificity of human UDP-glucuronosyltransferases in the glucuronidation of estriol, 16-epiestriol, 17-epiestriol, and 13-epiestradiol, Drug Metabol. Dispos.: the biological fate of chemicals 41 (3) (2013) 582–591, https://doi.org/10.1124/dmd.112.049072.
[46] F. Guengerich, M. Waterman, M. Egli, Recent structural insights into cytochrome P450 function, Trends Pharmacol. Sci. 37 (8) (2016) 625–640, https://doi.org/10.1016/j.tips.2016.05.006.
[47] M. Schwab, Cytochrome P450 enzymes in drug metabolism: regulation of gene expression, enzyme activities, and impact of genetic variation, Pharmacol. Therapeut. 138 (1) (2013) 103–141, https://doi.org/10.1016/j.pharmthera.2012.12.007.
[48] Omura Tsuneo, Forty years of cytochrome P450, Biochem. Biophys. Res. Commun. (1999), https://doi.org/10.1006/bbrc.1999.1887.
[49] J.A. Hasler, R. Estabrook, M. Murray, I. Pikuleva, M. Waterman, J. Capdevila, V. Holla, C. Helvig, J.R. Falck, G. Farrell, Human cytochromes P450, Mol. Aspect. Med. 20 (3) (1999) 1–137, https://doi.org/10.1016/S0098-2997(99)00005-9.